Bimodal Recurrence Pattern of Tsunamis in South-Central Chile: A Statistical Exploration of Paleotsunami Data

by Philipp Kempf, Jasper Moernaut, and Marc De Batist

ABSTRACT

To improve tsunami hazard assessment, paleotsunami research aims at extending the time span of a region's historical tsunami record to provide a greater number of interevent periods to investigate. With 17 tsunami deposits, that is, 16 interevent periods, the sedimentary record of Lake Huelde in south-central Chile belongs to the longest paleotsunami records from a coastal subduction zone setting. The compiled interevent periods of the Lake Huelde paleotsunami record show a complex bimodal recurrence pattern. The null hypothesis that the underlying process is a time-independent (memoryless) Poissonian process can be rejected by use of the Cox and Oakes test for exponentiality. By creating six different synthetic recurrence patterns based on statistical principles and real-world examples, we explore the reliability of simple descriptive statistical metrics. The results reveal that the level of certainty for mean interevent period or variability of the process varies strongly with sample size and underlying process, for example, rupture behavior. Of the investigated recurrence patterns, the simplest, that is, a normal distribution, is described with reasonable reliability with only three interevent periods. The required number of interevent periods needed increases with recurrence pattern complexity and/or time independence, that is, the most complex model is a supercycle model, which reaches the same level of reliability only after 100 interevent periods. We argue that the current best practice of reporting the mean interevent period with 1σ or 2σ ranges of the sample can be misleading for tsunami or seismic hazard assessment without considering the sample size and the possible underlying process. This becomes strikingly obvious when considering that the mean interevent period of the Lake Huelde record of ~325 yrs coincides with the antimode at ~315 yrs, that is, the least likely between the two modes of 115 and 490 yrs. The implications for south-central Chile are that the probability for a tsunami in the next 50 yrs is 11.6%, which decreases to only 5.2% if 250 yrs elapse without tsunami occurrence. This decrease in probability would be unaccounted for with a classical hazard assessment, for example, assuming Poissonian behavior. We conclude with four requisites for a robust recurrence pattern: (1) good age control, (2) a stable sensitivity of the record to be impacted by and preserve traces of the event, (3) continuity in the record, and (4) a sufficient sample size given the expected underlying process.

Electronic Supplement: Tables of statistic parameters of the synthetics.

INTRODUCTION

Modern tsunami risk mitigation plans are based on the results of probabilistic tsunami hazard assessments (PTHAs), in which tsunami source parameters are defined and a recurrence probability model is applied to the source (Geist and Parsons, 2006; Geist and Lynett, 2014). So far, tsunami sources, in the case of seismic triggering, have usually been modeled to recur time independently from previous earthquakes, that is, with a constant hazard rate, using a Poisson process. It has been recognized, however, that tsunami generation may have a more complex recurrence pattern, that is, supercycle fault rupture behavior among others (e.g., Sieh *et al.*, 2008), in which cases the used PTHAs may thus be deficient.

The Poisson process is widely used because of its time independency. Time-independent behavior means that the probability of a future event is unaffected by how much time has passed since the last event, that is, a memoryless process (conceptually important). It is easy to compute because it only needs a single parameter (the mean) as input to be complete. There are several systems in earthquake-related sciences in which Poissonian behavior is observed, for example:

1. rapid stress recovery after giant earthquakes indicates the potential of virtually time-independent, that is, Poissonian, earthquake occurrence on some subduction zones (Tormann *et al.*, 2015);
2. the earthquake catalog suggests Poissonian behavior of global **M** 9 earthquakes (McCaffrey, 2008); and
3. seismoturbidites in Lake Tutira, New Zealand, exhibit a Poissonian recurrence pattern (Gomez *et al.*, 2015).

 doi: 10.1785/0220180204

Contrastingly, indications for non-Poissonian behavior for tsunami generation and related processes have been observed in a number of settings, which offer other plausible scenarios in direct competition to the Poissonian model. For example:

1. subduction zones with wide seismogenic zones may rupture time dependently, in supercycles (Goldfinger *et al.*, 2013; Herrendörfer *et al.*, 2015), that is, a sequence of earthquakes in short succession is followed by an outsized earthquake;
2. earthquakes in West Sumatra exhibit a different type of supercycles (Sieh *et al.*, 2008; Philibosian *et al.*, 2017), that is, a sequence of earthquakes in short succession is followed by a long quiescent phase with a mean interval of 51.0 ± 61.4 yrs and a coefficient of variance (COV) of 1.20;
3. major subduction zone earthquakes on the Japan trench appear to occur a-periodically (Sawai *et al.*, 2009), that is, interevent periods ranging from 100 to 800 yrs with a mean interevent periods of 323.6 ± 185.7 yrs and 322.3 ± 224.4 yrs with COVs of 0.57 and 0.70, respectively;
4. major earthquakes on an isolated transform plate boundary appear to occur regularly (Berryman *et al.*, 2012), that is, with a mean interval of 329 ± 68 yrs with a COV of 0.33;
5. larger earthquakes in Chile appear to occur more periodically (Moernaut *et al.*, 2018), that is, with a mean interval of 291.8 ± 92.9 yrs with a COV of 0.32; and
6. major subduction zone earthquakes in Alaska appear to occur periodically (Shennan *et al.*, 2014), that is, with a mean interval of 594.0 ± 156.1 yrs with a COV of 0.26.

The descriptive statistical terminology, for example, supercycles, periodically, a-periodically, or regularly, used for recurrence patterns in the cited publications is unavoidably vague as is the terminology in this publication, because threshold values are not clearly defined. Another source of potential confusion is that mean interevent periods are reported in scientific publications with small sample sizes because they are the best available estimate. However, the usually reported standard deviation (or 2σ range) reflects the variability in the small dataset and not how well this value describes the inherent variability of the underlying process.

Historical documentation of tsunami occurrence is often used to constrain the mean recurrence interval of large tsunami inundations, improving hazard assessments. However, PTHAs with paleotsunami data with complex recurrence patterns as input do not yet exist. Incomplete or unreliable historical records and unaccounted variability in recurrence times could lead to costly overprotection of coastal areas or to an insufficiently prepared population exposed to a great hazard.

The geological approach to this problem of small sample sizes is to produce longer and continuous sedimentary records with dated event deposits. However, even most subduction zone paleoseismic and paleotsunami records are also too short, have inaccurate dating, or lack continuity to determine the variability in the recurrence pattern, with few exceptions, such as the seismoturbidite records from the Cascadia subduction zone (Goldfinger *et al.*, 2012) or the Hikurangi margin (Pouderoux *et al.*, 2012, 2014; Gomez *et al.*, 2015). The sensitivity of the depositional environment needs to be stable and low enough to record no unwanted sedimentary signals, for example, storms, but high enough to record each destructive tsunami. The environment also needs preservation potential for tsunami deposits, so that postdepositional processes do not rework the material. The best paleotsunami records in this regard have been produced from marshes (Cisternas *et al.*, 2005), beach ridges (Sawai *et al.*, 2009), coastal caves (Rubin *et al.*, 2017), and coastal lakes (Kelsey *et al.*, 2005; Kempf *et al.*, 2017) with 7–17 recorded tsunami inundations in a single record over several thousand years.

Here, we present a new and unusual recurrence pattern of the Lake Huelde paleotsunami record of 17 events in south-central Chile (Kempf *et al.*, 2017) and then discuss the statistical robustness of the findings in light of the completeness of the record and the rupture modes involved. By statistical modeling, we explore the effect of the underlying recurrence pattern on the required amount of interevent periods to describe the recurrence pattern reliably.

PREVIOUS WORK: 17 TSUNAMI DEPOSITS IN LAKE HUELDE, CHILE

Lake Huelde is located 1.3 km landward of the west coast of Chiloé Island, Chile, the northernmost Patagonian Island on the South American west coast and situated in the center of the 1960 C.E. Great Chilean earthquake (**M** 9.5) rupture zone (Fig. 1a).

A deposit of the associated tsunami was recognized in a lacustrine sediment sequence from Lake Huelde as a mostly sandy layer with intervals of mud rip-up clasts in a matrix of sand with a fine-grained mud cap at the top (Kempf *et al.*, 2015). In the deeper sedimentary record of Lake Huelde, similar sedimentary units were identified and interpreted as tsunami deposits, too (Fig. 1b,c; Kempf *et al.*, 2017). The tsunami sizes recorded in the sedimentary record of Lake Huelde range from tsunamis that wash over ~6–m–high dunes to small tsunamis that are merely reaching the lake through the river channel (Kempf *et al.*, 2015, 2017). Tsunamis that do not reach the lake, though potentially posing a small, local hazard, are beyond the sensitivity limit of the record.

Radiocarbon dates provided the main source for input for two models that describe the age–depth relationship in the sediment cores (Figs. 1c and 2; Ⓔ Table S1, available in the electronic supplement to this article; Kempf *et al.*, 2017); one was created with the Bayesian, autoregressive accumulation rate age–depth modeling algorithm called BACON based in an R environment (Blaauw and Christen, 2011), the other with the standalone Bayesian age–depth model algorithm called P_Sequence of the OxCal family (Bronk Ramsey, 2008).

Both models were in agreement with each other without showing any model-specific artifacts. Probabilistic ages were modeled for each tsunami deposit creating a paleotsunami

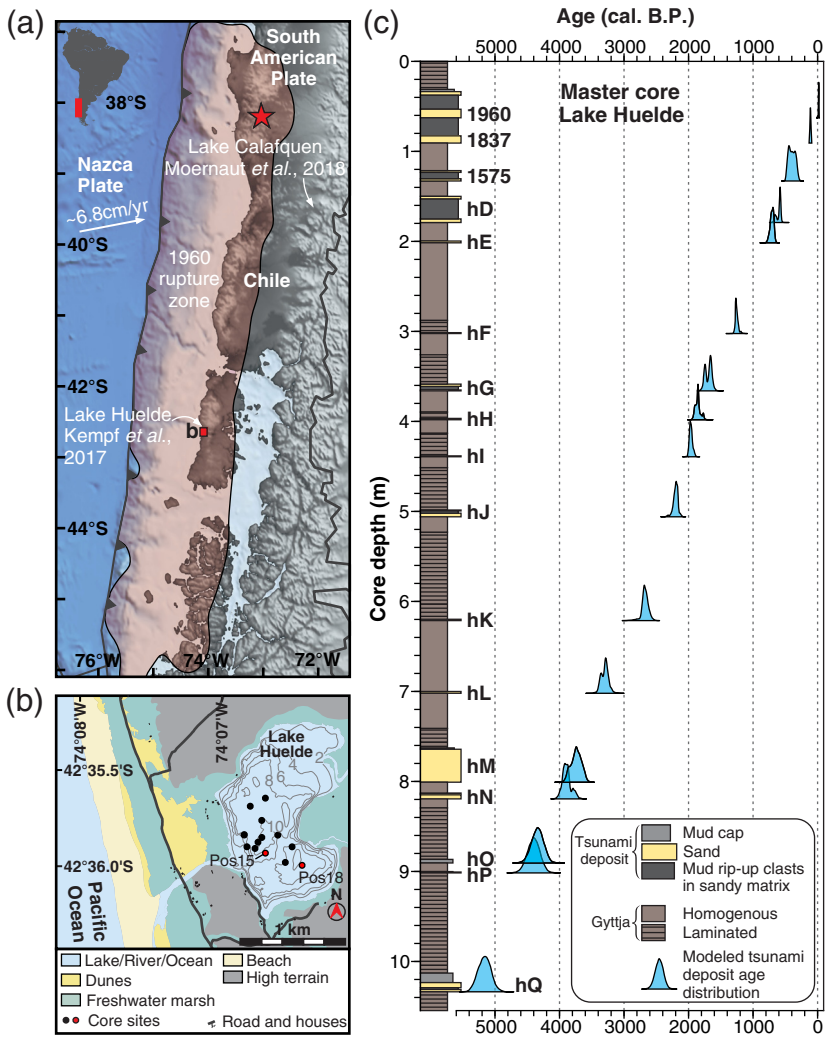

▲ **Figure 1.** (a) Overview map of south-central Chile with Lake Huelde located in the middle of the 1 m slip isoline of the 1960 Great Chilean earthquake rupture (transparent overlay; Moreno *et al.*, 2009); (b) geomorphological map of Lake Huelde near the Pacific coastline on Chiloé Island (Kempf *et al.*, 2017); (c) master core of the Lake Huelde sedimentary record with all tsunami deposits and their modeled ages (Kempf *et al.*, 2017). The abbreviations for the event deposits (hD, hE, and so on) stand for Lake Huelde (h) and a capital letter in alphabetical order with increasing age. The color version of this figure is available only in the electronic edition.

record of the last 5500 yrs. The Lake Huelde sedimentary record is the longest paleotsunami record on the entire Peru–Chile subduction zone and is in strong agreement with the previously known paleotsunami record of the past 2000 yrs without any overrepresentation or underrepresentation (Kempf *et al.*, 2017). The lacustrine sediment sequence appears to be continuous and the age control is good throughout the entire record. At present, the Lake Huelde record should be the most reliable record in the region for paleotsunami recurrence pattern reconstruction. The Lake Huelde record bears evidence of nine previously unknown tsunamis.

METHODS

We use the results of Kempf *et al.* (2017; Ⓔ Table S1) to compute the modeled interevent period between each tsunami deposit (Figs. 1 and 2). In BACON, two consecutive tsunami deposit ages within each of the Markov chain Monte Carlo iterations can be elegantly subtracted from each other to get a probabilistic description of an interevent period between the two tsunamis. Age reversals (i.e., negative interevent periods) and artificially narrower or wider interevent period distributions are avoided this way. In OxCal, we used the Difference()-function, which is designed for the same purpose (Fig. 2).

First, we test for the null hypothesis of a Poisson process in the Lake Huelde paleotsunami record using the Cox and Oakes test for exponentiality. The Cox and Oakes test is one of several tests for exponentiality, but among those it has proven to be relatively powerful, if not the best, when no further information about the dataset is known, and seems to be relatively successful with smaller sample numbers (Ascher, 1990; Rahman and Wu, 2017). Essentially, the result of the Cox and Oakes test of exponentiality can reject the hypothesis of exponentiality for a dataset for both small and large results of the deviate (Fig. 3; Cox and Oakes, 1984).

Second, we simulate records, sourced from six created recurrence patterns (also tested for exponentiality for reference; Fig. 3), which are a mixture of conceptual distributions (Poissonian recurrence, Gaussian recurrence, uniform recurrence) and real-world examples (exponential power model for large-scale earthquakes observed in Chilean lakes, e.g., Moernaut *et al.*, 2018; Huelde model for tsunamis observed in coastal Lake Huelde, south-central Chile, e.g., Kempf *et al.*, 2017; and supercycle model for megathrust earthquakes on the Sunda arc in north Sumatra, e.g., Sieh *et al.*, 2008; Philibosian *et al.*, 2017). From the simulated records, we sample synthetic sedimentary event records of 3, 6, 10, 16, 30, and 100 interevent periods and analyze the statistical robustness of the conclusions that would be drawn from these records.

For the Cox and Oakes test and its visualization, we use the R environment and the "exptest" library (Novikov *et al.*, 2013). The statistical modeling, its description, and its visualization were written in generic R language.

The results of this study are expressed in frequency distributions. The frequencies are often not normally distributed, which is why we will not express these results in 1σ and 2σ ranges. The interquartile range (IQR) is typically used instead,

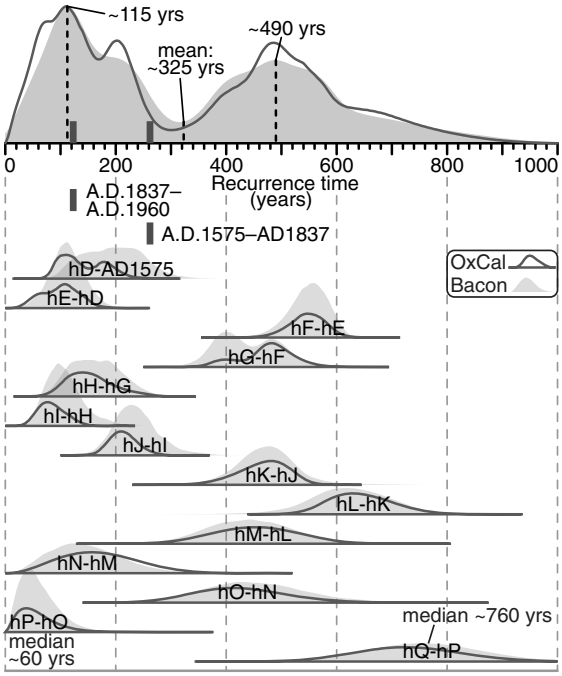

▲ **Figure 2.** Age-depth modeled recurrence pattern of tsunami deposits in the sedimentary record of Lake Huelde. Each interevent period, for example, between events hK and hJ, from young (top) to old (bottom). The overall recurrence pattern is shown on top. The solid line expresses the results of the OxCal P_Sequence and the gray areas show the results of BACON. No significant model-specific artifacts were observed. For ease of use, we continued with the R-based BACON results.

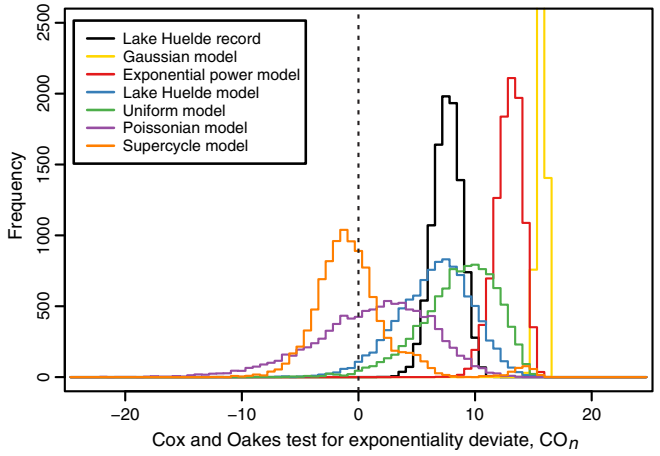

▲ **Figure 3.** The Lake Huelde sedimentary record (distribution with a peak at $CO_n = 8$) is tested for exponentiality using the Cox and Oakes test (Cox and Oakes, 1984). For all 10,000 samples of the record the deviate CO_n of the Cox and Oakes test is greater than 0, which means exponentiality, that is, the Poissonian process, can be excluded for Lake Huelde tsunami deposits. The Cox and Oakes test was repeated for all synthetic models. Except for the Poissonian and the supercycle models, all models failed the test for exponentiality. The color version of this figure is available only in the electronic edition.

that is, the difference between the 25th and 75th percentiles. To keep a reference to the often used 1σ and 2σ ranges, we will present the 68% and 95% confidence ranges. They are the same type of data as the IQR except with boundaries at the 2.5%, 16%, 84%, and 97.5% quantiles.

TESTING FOR THE NULL HYPOTHESIS OF POISSONIAN BEHAVIOR

The computed mean interevent period of tsunamis that reach Lake Huelde is 325 yrs, which is comparable to conclusions drawn from other records of this region (Cisternas *et al.*, 2005, 2017). However, the recurrence pattern is strongly bimodal (Fig. 2). The first and narrower mode is at 115 yrs and the second and wider mode is at 490 yrs.

Despite the obvious visual discrepancy of the Lake Huelde recurrence pattern and a generic exponential distribution, we will apply the Cox and Oakes test for exponentiality (Cox and Oakes, 1984) by simulating 10,000 sets of 16 interevent periods based on the results from the probabilistic ages of tsunami deposits from the BACON algorithm (Blaauw and Christen, 2011) in the sedimentary record of Lake Huelde (Kempf *et al.*, 2017). All 10,000 sets of simulated records are put through the Cox and Oakes test for exponentiality and the results are plotted as a histogram (Fig. 3, black line). The histogram of the test result of the Lake Huelde dataset is entirely offset from 0 toward greater numbers and therefore we can reject the null hypothesis of exponentiality of tsunami inundation in the Lake Huelde dataset.

Because all tsunami deposits in Lake Huelde are suggested to be from near-field tsunamis (Kempf *et al.*, 2017), it appears that the tsunamigenic earthquakes on the seismic segment of the 1960 rupture zone are not time independent.

INTEREVENT PERIOD MODELING

For south-central Chile, the question remains, whether 16 interevent periods are enough to draw a statistically robust conclusion from a dataset toward the overall recurrence pattern. To assess the reliability of geological records of events, which often suffer from low sample number, we created six recurrence models, that is, Gaussian, exponential power, Lake Huelde, uniform, Poissonian, and supercycle models (Fig. 4a; Ⓔ Table S2). They are all scaled to have a mean interevent period of 100 yrs. However, the time unit is interchangeable, so that it can be applied to studies of other events, for example, volcano eruptions, floods, tropical cyclones, glacial lake outburst floods, glacier surges, etc. When a specific comparison is made to a real-world example it is the shape of the distribution that is meant, not the absolute values. The models are described below and the COV is stated to compare with several statistical analyses in the literature (Fig. 4a; Kulkarni *et al.*, 2013; Moernaut *et al.*, 2018):

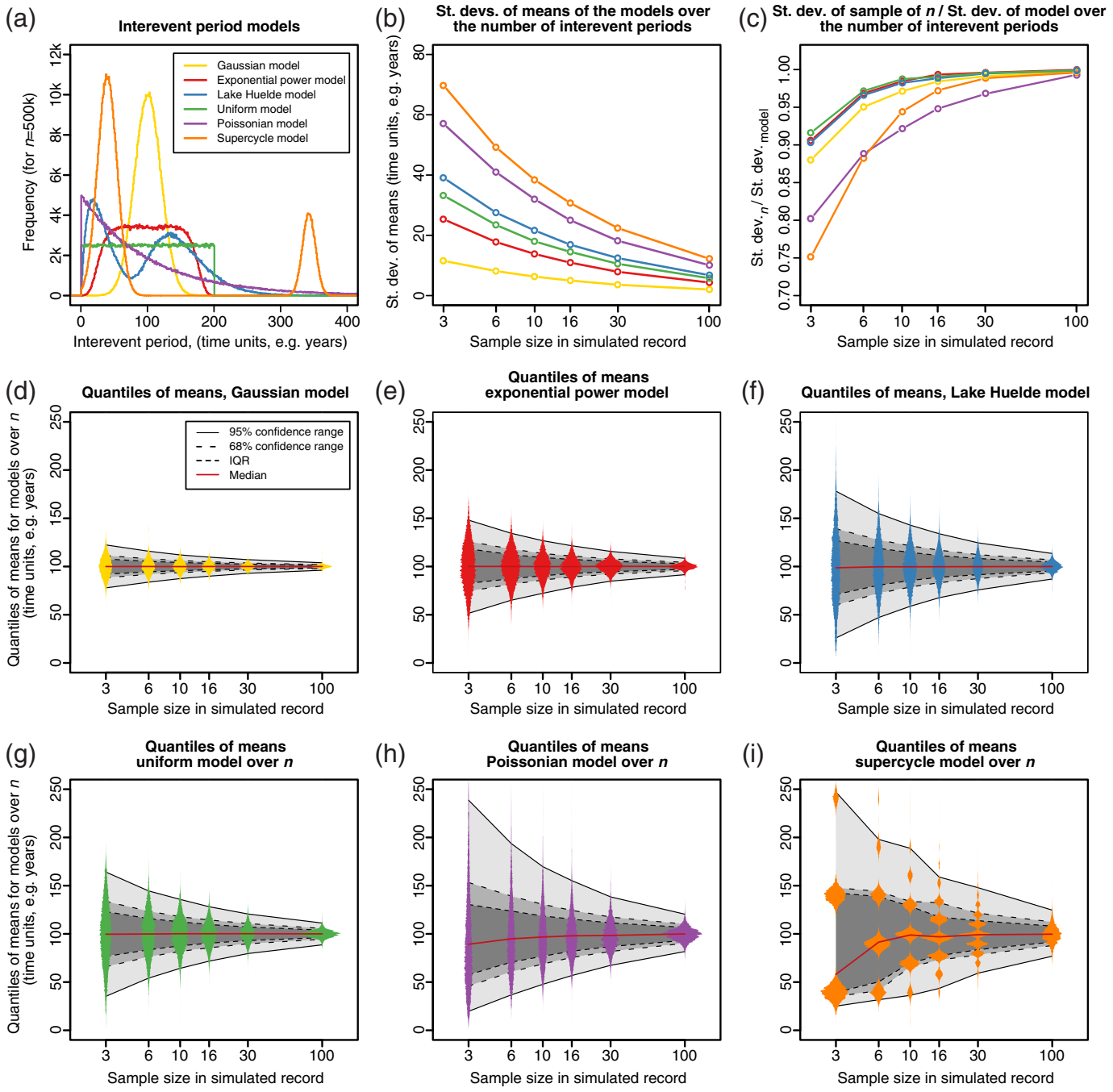

▲ **Figure 4.** (a) Six synthetic recurrence models, all scaled to have a mean of 100 yrs; (b) the standard deviation is used to describe how the accuracy of the mean interevent period of a dataset changes depending on the number of samples that are considered; (c) description of how the standard deviation of a dataset approaches the standard deviation of the underlying process; (d–i) illustration of how the accuracy of descriptive statistics on datasets change with sample size for the six synthetic models. Compared across the models, the Gaussian model can be accurately described with the lowest sample number. The Poissonian and supercycle models need the greatest sample numbers for accurate statistic description. The color version of this figure is available only in the electronic edition.

1. Gaussian model: a normally distributed recurrence pattern with the mean of 100 yrs and the standard deviation of 20 yrs. The COV is 0.20. Example: megathrust earthquakes in Alaska (Shennan *et al.*, 2014), in this case six interevent periods.

2. Exponential power model: we choose an exponential power distribution to produce a model between the normal distribution and a uniform distribution, that is, a normal distribution with a plateau. It is defined by the mean, a scaling parameter α, and a shape parameter β. If the shape

parameter $\beta = 1$, it produces a Laplace distribution; if $\beta = 2$ it is a normal distribution; if $\beta = \infty$ it is a uniform distribution. We choose $\beta = 8$. The COV in this case is 0.44. Example: seismoturbidites from Lake Calafquen (Fig. 1; Moernaut *et al.*, 2018), in this case 12 interevent periods.

3. Huelde model: this composite model consists of two gamma distributions with similar shape parameters ($k_1 = 1.7$ and $k_2 = 1.75$), but with a constant shift of the second distribution toward longer interevent periods. The COV is 0.68. This case is specifically constructed to mimic the recurrence pattern found in Lake Huelde based on 16 interevent periods (Kempf *et al.*, 2017).
4. Uniform model: this model has an even probability within the range of 200 yrs. Within its extremes, it is identical to a random number generator. The COV is 0.58. This model was chosen for a statistical benchmark, not for its real-world potential and has to our knowledge no real-world example within the geosciences.
5. Poissonian model: this model is based on an exponential distribution. It is synonymous with time-independent interevent periods. This model was included because of its tremendous real-world use, with a COV of 1.00. Example: seismoturbidites in Lake Tutira, New Zealand (Gomez *et al.*, 2015), in this case 118 and 24 interevent periods.
6. Supercycle model: this composite model consists of two normal distributions, where shorter interevent periods (mean = 40 and standard deviation = 15) occur four times as often as longer interevent periods (mean = 340 and standard deviation = 50). The COV is 1.225. Example: subduction zone earthquakes on the Sunda arc (Sieh *et al.*, 2008; Philibosian *et al.*, 2017), in this case 13 interevent periods.

To compare the simulated records with the Lake Huelde record, we applied the Cox and Oakes test for exponentiality on each of the simulated records. All but the Poissonian and the supercycle models have low or no counts in the histogram bins around $CO_n \approx 0$, in which CO refers to Cox and Oakes deviate (Fig. 3). The Cox and Oakes test seems to lack the power to recognize the supercycle model as non-Poissonian; however, there exists a small mode around $CO_n = 14$, which would look peculiar if one were to test a supercycle dataset for exponentiality (Fig. 3).

On the basis of all six models, we simulated 10,000 records each for sample sizes of 3, 6, 10, 16, 30, and 100 interevent periods (Fig. 4a). The greater the sample size of interevent periods the lower the standard deviation of the mean interevent periods (Fig. 4b) and the closer the standard deviation of the simulated records to the standard deviation of the underlying recurrence model (Fig. 4c). How well the simulated records estimate mean, median, and the 68% and 95% confidence ranges over sample size is described for each model separately (Fig. 4d–i; Ⓔ Table S2). For both the Poissonian model and the supercycle model, the mean recurrence is exceptionally badly estimated for sample sizes of 3 (68% confidence range is 58 and 71 yrs, respectively), 6 (68% confidence range is 41 and 50 yrs, respectively), and 10 interevent periods (68% confidence range is 32 and 39 yrs, respectively) (Ⓔ Table S2; Fig. 4h,i). The standard deviations of the Poissonian model and the supercycle model become possible to be estimated with 95% certainty only beyond a sample size of 16 and 10, respectively (Fig. 4c). This result in certainty level versus sample size in the Poissonian model is comparable with the necessary sample size of >20 to estimate the variability in a Poissonian process with a 95% certainty (McCaffrey, 2008). Across all six models of recurrence patterns, the Poissonian model is the most difficult to estimate if certainty levels above 90% are needed on the variability of interevent periods.

Under the assumption that the resulting recurrence pattern of tsunamis inundating Lake Huelde (Fig. 2) is correct, the Lake Huelde record should be interpreted to be within 17% (55 yrs in the case of Lake Huelde) and 33% (107 yrs) of the mean with 68% and 95% confidence ranges, respectively (Fig. 4f).

Approaching the statistical model results from a planning point of view of a geoscientist, one could say that if the investigated process is expected to be similar to the Huelde model, then the result should be within the 68% confidence range of the real process with ~88% certainty with a sample size of 16. If the investigated process is expected to be similar to the Gaussian model, then the result should be within the 68% confidence range of the real process with ~88% certainty with a sample size of only 3. From a civil authorities point of view, to achieve an 80% certainty to be within the 68% confidence range of the model, one would need $n \geq 3$ for the Gaussian model, $n > 3$ for the exponential power model, $n > 6$ for the uniform model, $n > 10$ for the Huelde model, $n > 16$ for the Poissonian model, and $n > 30$ for the supercycle model (Ⓔ Table S2).

RECURRENCE PATTERN OF TSUNAMIS IN SOUTH-CENTRAL CHILE

The first mode of the bimodal recurrence pattern at 115 yrs (Fig. 2) is comparable to the historical 128 ± 31 yrs mean recurrence time of megathrust earthquakes in the same region (Lomnitz, 1970, 2004; Nishenko, 1985), whereas the second mode at 490 yrs is in agreement with the expected 500 yrs recurrence time of full segment ruptures with patches of 40 m of slip, such as the 1960 C.E. earthquake (Cifuentes, 1989; Moreno *et al.*, 2009; Moernaut *et al.*, 2014). More recent findings of two separate and time-dependent earthquake recurrence patterns in the 1960 C.E. rupture zone suggest recurrence times of 139 ± 69 yrs and 292 ± 93 yrs for **M** ≥ 7.7 and **M** ≥ 8.6 earthquakes, respectively (Moernaut *et al.*, 2018). In the Lake Huelde record, we cannot make a distinction between earthquake or tsunami magnitudes, because the tsunami deposits can exhibit strong spatial variability (Kempf *et al.*, 2015).

The bimodality of the recurrence pattern of tsunamis inundating Lake Huelde is statistically robust. The bimodality can be explained in three different ways. First, data may be missing. This seems unlikely, due to the strong agreement between the Lake Huelde record and the historical and sedimentary records during the last ~2000 yrs from other areas without

overrepresentation or underrepresentation (Kempf *et al.*, 2017). Furthermore, the youngest eight tsunami deposits of the last ~2000 yrs from Lake Huelde can be correlated to coastal subsidence, and therefore to near-field events in Maullín, 110 km north of Lake Huelde (Fig. 1; Cisternas *et al.*, 2005).

Second, meteorite impacts, purely landslide related and other triggers as tsunamigenic processes could superimpose and cause bimodality. These triggers can be excluded because there are no known candidates, and should they have occurred in the past 5500 yrs, it would most likely be a singular event in the record. It is possible that far-field tsunamis from other subduction zone segments across the Pacific are among the tsunami sources. However, in recent history, for example, 1946 C.E. Aleutian Islands, 1952 C.E. Kamchatka, 1964 C.E. Alaska, 2010 C.E. Maule, and 2011 C.E. Tōhoku, none of the giant Pacific tsunamis caused inundation into Lake Huelde or had a significant effect elsewhere on the coast of Chiloé Island. If tsunami deposits with far-field sources exist in the Lake Huelde record, it would make the recurrence of local tsunamigenic earthquakes longer. However, the hazard emanating from extreme waves—far field or near field—on the south-central Chilean coast would remain the same.

Third, the tsunamigenic earthquakes may be a process that is inherently bimodal in south-central Chile, controlled by temporal and spatial variability in multiple rupture modes on the megathrust. The various rupture modes could have unimodal recurrence patterns. This appears to be the most plausible hypothesis, because of precedence in south-central Chile and on other subduction zones.

The seismic rupture potential related to the megathrust in south-central Chile varies along strike and down-dip. The along-strike variations are controlled by asperities of various sizes with various interevent periods (Moreno *et al.*, 2018) causing along-strike segmentation, often following patterns of interseismic coupling, for example, on the Peru–Chile (Moreno *et al.*, 2011), the Sunda arc (Chlieh *et al.*, 2008), and the Kamchatka subduction zones (Bürgmann *et al.*, 2005). In south-central Chile, the down-dip zonation is inferred to be controlled by fluid pressure originating from the slab to Moho contact zone influencing the deepest seismogenic zone to be able to rupture with shorter interevent periods (~60 yrs) and lower magnitude (**M** 7–8) compared to the shallower seismogenic zone (> 110 yrs; **M** 8–9; Moreno *et al.*, 2018). Both along-strike and down-dip segmentations can be overcome in great 1960-style earthquakes (Moreno *et al.*, 2018) causing giant trans-Pacific tsunamis.

Further variations in tsunami generation could stem from splay fault ruptures, which have been documented on the Chilean subduction zone around Santa Maria Island (Melnick *et al.*, 2012), and which tend to be very tsunamigenic (Moore *et al.*, 2007). Tsunami earthquakes that rupture only the most up-dip zone of the megathrust with comparatively low magnitude but high tsunamigenic potential such as the 2010 Mentawai rupture on the Sunda arc (Lay *et al.*, 2011) have not been recorded on the Chilean subduction zone so far. We interpret the varying and possibly complex recurrence patterns of each of these processes on or near the megathrust to control the overall bimodal recurrence pattern of tsunamis that inundated Lake Huelde.

Classifying the earthquake of each tsunami deposit would allow an analysis of the recurrence patterns of separate rupture modes. However, additional paleoseismic information to estimate rupture width and length, location, and slip distribution would be needed for that. This information may be acquired by integrating this and other paleotsunami and paleoseismological records with new long records of shaking and coastal deformation.

IMPLICATIONS FOR HAZARD ASSESSMENT

The mean recurrence time loses meaning for hazard assessment in face of strongly bimodal recurrence patterns of tsunamigenic subduction zone earthquakes. In fact, in the case of tsunami inundation in Lake Huelde the mean is close to the antimode at 315 yrs, that is, the least likely recurrence time between the two modes. The implications of the recurrence pattern are clear. The shortest recurrence period in Lake Huelde has a median of ~60 yrs. Similar to Moreno *et al.* (2011) and Moernaut *et al.* (2018), we find in the Lake Huelde record that the subduction zone in south-central Chile may already have the potential to produce a tsunamigenic earthquake.

The probability of an event in the next 50 yrs with the Lake Huelde record recurrence pattern is at 11.6%. This compares well to 14.4% when assuming Poissonian behavior with the mean derived from the Lake Huelde record, and it deviates from 5.6% when assuming a normal distribution with a mean and standard deviation derived from the Lake Huelde record. However, assuming no event occurs in the next 250 yrs, the probability for a tsunami in the next 50 yrs, that is, in the period from 308 to 358 yrs after the last event, is much lower with the Lake Huelde recurrence pattern at 5.2%, which in turn is much lower than the probabilities for a tsunami in the same period for a Poissonian process at 14.4% and a normally distributed process at 17.7%.

In terms of hazard assessment and risk management in south-central Chile, we would argue against the current best practice to report mean interevent periods as a measure for tsunami hazard. Considering that many subduction zones lack sufficient evidence for simple recurrence patterns, it should be best practice in any region to express mean interevent periods with an assessment of the most likely underlying process distribution, for example, subduction zone earthquakes occur periodically with a mean interevent period of 594 ± 156 yrs in south Alaska (Shennan *et al.*, 2014).

The statistical exploration of the interevent period data has shown that there are vast differences in the required number of interevent periods dependent on the underlying process. As we cannot know the underlying process from low sample size records, we would advise caution when deriving mean interevent periods from a few interevent periods. This conclusion can be expanded geographically beyond south-central Chile and to various recurring phenomena because other processes than tsunamis and large earthquakes behave this way. However,

if the investigated process falls within the spectrum of recurrence patterns presented here (Fig. 4a), then the prerequisites for a robust recurrence pattern analysis are (a) good age control, (b) a stable sensitivity of the record to be impacted by and preserve traces of the event, (c) continuity in the record, and finally (d) a sufficient sample size given the expected underlying process.

DATA AND RESOURCES

All data used were taken from published references. The sediment cores, the prior age information (mostly radiocarbon dates), and the BACON- and OxCal-based age depth models were taken from Kempf *et al.* (2017). The Cox and Oakes exponentiality test code was taken from Novikov *et al.* (2013). The rest of the code for this study was written in the R environment by the authors.

ACKNOWLEDGMENTS

P. K. acknowledges financial support by the Special Research Fund of Ghent University (BOF). The authors thank Mario Pino and Roberto Urrutia for facilitating the fieldwork; the authors thank Koen De Rycker, Maarten Van Daele, Willem Vandoorne, and Gauvain Wiemer for help during fieldwork. The authors thank Maarten Van Daele for fruitful discussions. They also thank two anonymous reviewers for their valuable input.

REFERENCES

Ascher, S. (1990). A survey of tests for exponentiality, *Comm. Stat. Theor. Meth.* **19,** no. 5, 1811–1825, doi: 10.1080/03610929008830292.

Berryman, K. R., U. A. Cochran, K. J. Clark, G. P. Biasi, R. M. Langridge, and P. Villamor (2012). Major earthquakes occur regularly on an isolated plate boundary fault, *Science* **336,** no. 6089, 1690–1693, doi: 10.1126/science.1218959.

Blaauw, M., and J. A. Christen (2011). Flexible paleoclimate age-depth models using an autoregressive gamma process, *Bayesian Anal.* **6,** no. 3, 457–474, doi: 10.1214/11-BA618.

Bronk Ramsey, C. (2008). Deposition models for chronological records, *Quaternary Sci. Rev.* **27,** nos. 1/2, 42–60, doi: 10.1016/j.quascirev.2007.01.019.

Bürgmann, R., M. G. Kogan, G. M. Steblov, G. Hilley, V. E. Levin, and E. Apel (2005). Interseismic coupling and asperity distribution along the Kamchatka subduction zone, *J. Geophys. Res.* **110,** no. B7, doi: 10.1029/2005JB003648.

Chlieh, M., J. P. Avouac, K. Sieh, D. H. Natawidjaja, and J. Galetzka (2008). Heterogeneous coupling of the Sumatran megathrust constrained by geodetic and paleogeodetic measurements, *J. Geophys. Res.* **113,** no. B5, doi: 10.1029/2007JB004981.

Cifuentes, I. L. (1989). The 1960 Chilean earthquakes, *J. Geophys. Res.* **94,** no. B1, 665–680, doi: 10.1029/JB094iB01p00665.

Cisternas, M., B. F. Atwater, F. Torrejón, Y. Sawai, G. Machuca, M. Lagos, A. Eipert, C. Youlton, I. Salgado, T. Kamataki, *et al.* (2005). Predecessors of the giant 1960 Chile earthquake, *Nature* **437,** no. 7057, 404–407, doi: 10.1038/nature03943.

Cisternas, M., E. Garrett, R. Wesson, T. Dura, and L. L. Ely (2017). Unusual geologic evidence of coeval seismic shaking and tsunamis shows variability in earthquake size and recurrence in the area of the giant 1960 Chile earthquake, *Mar. Geol.* **385,** 101–113, doi: 10.1016/j.margeo.2016.12.007.

Cox, D. R., and D. Oakes (1984). *Analysis of Survival Data*, Chapman and Hall, London, United Kingdom.

Geist, E. L., and P. J. Lynett (2014). Source processes for the probabilistic assessment of tsunami hazards, *Oceanography* **27,** no. 2, 86–93, doi: 10.5670/oceanog.2014.43.

Geist, E. L., and T. Parsons (2006). Probabilistic analysis of tsunami hazards, *Nat. Hazards* **37,** no. 3, 277–314, doi: 10.1007/s11069-005-4646-z.

Goldfinger, C., Y. Ikeda, R. S. Yeats, and J. Ren (2013). Superquakes and supercycles, *Seismol. Res. Lett.* **84,** no. 1, 24–32, doi: 10.1785/0220110135.

Goldfinger, C., C. H. Nelson, A. E. Morey, J. E. Johnson, J. R. Patton, E. Karabanov, J. Gutiérrez-Pastor, A. T. Eriksson, E. Gràcia, G. Dunhill, *et al.* (2012). Turbidite event history—Methods and implications for Holocene paleoseismicity of the Cascadia subduction zone, *U.S. Geol. Surv. Profess. Pap. 1661-F,* 170 pp.

Gomez, B., Á. Corral, A. R. Orpin, M. J. Page, H. Pouderoux, and P. Upton (2015). Lake Tutira paleoseismic record confirms random, moderate to major and/or great Hawke's Bay (New Zealand) earthquakes, *Geology* **43,** no. 2, 103–106, doi: 10.1130/G36006.1.

Herrendörfer, R., Y. van Dinther, T. Gerya, and L. A. Dalguer (2015). Earthquake supercycle in subduction zones controlled by the width of the seismogenic zone, *Nature Geosci.* **8,** no. 6, 471–474.

Kelsey, H. M., A. R. Nelson, E. Hemphill-Haley, and R. C. Witter (2005). Tsunami history of an Oregon coastal lake reveals a 4600 yr record of great earthquakes on the Cascadia subduction zone, *Geol. Soc. Am. Bull.* **117,** no. 7, 1009–1032, doi: 10.1130/B25452.1.

Kempf, P., J. Moernaut, M. Van Daele, W. Vandoorne, M. Pino, R. Urrutia, and M. De Batist (2017). Coastal lake sediments reveal 5500 years of tsunami history in south central Chile, *Quaternary Sci. Rev.* **161,** 99–116, doi: 10.1016/j.quascirev.2017.02.018.

Kempf, P., J. Moernaut, M. Van Daele, F. Vermassen, W. Vandoorne, M. Pino, R. Urrutia, S. Schmidt, E. Garrett, and M. De Batist (2015). The sedimentary record of the 1960 tsunami in two coastal lakes on Isla de Chiloé, south central Chile, *Sediment. Geol.* **328,** 73–86, doi: 10.1016/j.sedgeo.2015.08.004.

Kulkarni, R., I. Wong, J. Zachariasen, C. Goldfinger, and M. Lawrence (2013). Statistical analyses of great earthquake recurrence along the Cascadia subduction zone, *Bull. Seismol. Soc. Am.* **103,** no. 6, 3205–3221, doi: 10.1785/0120120105.

Lay, T., C. J. Ammon, H. Kanamori, Y. Yamazaki, K. F. Cheung, and A. R. Hutko (2011). The 25 October 2010 Mentawai tsunami earthquake (M_w 7.8) and the tsunami hazard presented by shallow megathrust ruptures, *Geophys. Res. Lett.* **38,** no. 6, doi: 10.1029/2010GL046552.

Lomnitz, C. (1970). Major earthquakes and tsunamis in Chile during the period 1535 to 1955, *Geol. Rundsch.* **59,** 938–960.

Lomnitz, C. (2004). Major earthquakes of Chile: A historical survey, 1535–1960, *Seismol. Res. Lett.* **75,** no. 3, 368–378, doi: 10.1785/gssrl.75.3.368.

McCaffrey, R. (2008). Global frequency of magnitude 9 earthquakes, *Geology* **36,** no. 3, 263–266, doi: 10.1130/G24402A.1.

Melnick, D., M. Moreno, M. Motagh, M. Cisternas, and R. L. Wesson (2012). Splay fault slip during the M_w 8.8 2010 Maule, Chile earthquake, *Geology* **40,** no. 3, 251–254.

Moernaut, J., M. Van Daele, K. Fontijn, K. Heirman, P. Kempf, M. Pino, G. Valdebenito, R. Urrutia, M. Strasser, and M. De Batist (2018). Larger earthquakes recur more periodically: New insights in the megathrust earthquake cycle from lacustrine turbidite records in south-central Chile, *Earth Planet. Sci. Lett.* **481,** 9–19, doi: 10.1016/j.epsl.2017.10.016.

Moernaut, J., M. Van Daele, K. Heirman, K. Fontijn, M. Strasser, M. Pino, R. Urrutia, and M. De Batist (2014). Lacustrine turbidites as a tool for quantitative earthquake reconstruction: New evidence for a variable rupture mode in south central Chile, *J. Geophys. Res.* **119,** no. 3, 1607–1633, doi: 10.1002/2013JB010738.

Moore, G. F., N. L. Bangs, A. Taira, S. Kuramoto, E. Pangborn, and H. J. Tobin (2007). Three-dimensional splay fault geometry and implications for tsunami generation, *Science* **318,** no. 5853, 1128–1131, doi: 10.1126/science.1147195.

Moreno, M., S. Li, D. Melnick, J. R. Bedford, J. C. Baez, M. Motagh, S. Metzger, S. Vajedian, C. Sippl, B. D. Gutknecht, *et al.* (2018). Chilean megathrust earthquake recurrence linked to frictional contrast at depth, *Nature Geosci.* **11,** no. 4, 285–290, doi: 10.1038/s41561-018-0089-5.

Moreno, M., D. Melnick, M. Rosenau, J. Bolte, J. Klotz, H. Echtlera, J. Baez, K. Bataille, J. Chen, M. Bevis, *et al.* (2011). Heterogeneous plate locking in the south-central Chile subduction zone: Building up the next great earthquake, *Earth Planet. Sci. Lett.* **305,** nos. 3/4, 413–424, doi: 10.1016/j.epsl.2011.03.025.

Moreno, M. S., J. Bolte, J. Klotz, and D. Melnick (2009). Impact of megathrust geometry on inversion of coseismic slip from geodetic data: Application to the 1960 Chile earthquake, *Geophys. Res. Lett.* **36,** L16310, doi: 10.1029/2009GL039276.

Nishenko, S. P. (1985). Seismic potential for large and great interplate earthquakes along the Chilean and southern Peruvian margins of South America: A quantitative reappraisal, *J. Geophys. Res.* **90,** no. B5, 3589–3615, doi: 10.1029/JB090iB05p03589.

Novikov, A., R. Pusev, and M. Yakovlev (2013). exptest: Tests for exponentiality, *R Package Version 1.2*.

Philibosian, B., K. Sieh, J.-P. Avouac, D. H. Natawidjaja, H.-W. Chiang, C.-C. Wu, C.-C. Shen, M. R. Daryono, H. Perfettini, B. W. Suwargadi, *et al.* (2017). Earthquake supercycles on the Mentawai segment of the Sunda megathrust in the seventeenth century and earlier, *J. Geophys. Res.* doi: 10.1002/2016JB013560.

Pouderoux, H., G. Lamarche, and J.-N. Proust (2012). Building an 18,000-year-long paleo-earthquake record from detailed deep-sea turbidite characterisation in Poverty Bay, New Zealand, *Nat. Hazards Earth Syst. Sci.* **12,** no. 6, 2077–2101, doi: 10.5194/nhess-12-2077-2012.

Pouderoux, H., J.-N. Proust, and G. Lamarche (2014). Submarine paleoseismology of the northern Hikurangi subduction margin of New Zealand as deduced from turbidite record since 16 ka, *Quaternary Sci. Rev.* **84,** 116–131, doi: 10.1016/j.quascirev.2013.11.015.

Rahman, M., and H. Wu (2017). Tests for exponentiality: A comparative study, *Am. J. Appl. Math. Stat.* **5,** no. 4, 125–135, doi: 10.12691/ajams-5-4-3.

Rubin, C. M., B. P. Horton, K. Sieh, J. E. Pilarczyk, P. Daly, N. Ismail, and A. C. Parnell (2017). Highly variable recurrence of tsunamis in the 7,400 years before the 2004 Indian Ocean tsunami, *Nature Comm.* **8,** Article Number 16019, doi: 10.1038/ncomms16019.

Sawai, Y., T. Kamataki, M. Shishikura, H. Nasu, Y. Okamura, K. Satake, K. H. Thomson, D. Matsumoto, Y. Fujii, J. Komatsubara, *et al.* (2009). Aperiodic recurrence of geologically recorded tsunamis during the past 5500 years in eastern Hokkaido, Japan, *J. Geophys. Res.* **114,** no. B01319, doi: 10.1029/2007JB005503.

Shennan, I., R. Bruhn, N. Barlow, K. Good, and E. Hocking (2014). Late Holocene great earthquakes in the eastern part of the Aleutian megathrust, *Quaternary Sci. Rev.* **84,** 86–97, doi: 10.1016/j.quascirev.2013.11.010.

Sieh, K., D. H. Natawidjaja, A. J. Meltzner, C.-C. Shen, H. Cheng, K.-S. Li, B. W. Suwargadi, J. Galetzka, B. Philibosian, and R. L. Edwards (2008). Earthquake supercycles inferred from sea-level changes recorded in the corals of West Sumatra, *Science* **322,** no. 5908, 1674–1678.

Tormann, T., B. Enescu, J. Woessner, and S. Wiemer (2015). Randomness of megathrust earthquakes implied by rapid stress recovery after the Japan earthquake, *Nature Geosci.* **8,** no. 2, 152–158, doi: 10.1038/ngeo2343.

Philipp Kempf[1]
Geological Survey of Belgium
Royal Belgian Institute of Natural Sciences
Jennerstraat 13
1000 Brussels, Belgium
pkempf@naturalsciences.be

Jasper Moernaut
Institute of Geology
University of Innsbruck
Innrain 52
6020 Innsbruck, Austria
jasper.moernaut@uibk.ac.at

Marc De Batist
Renard Centre of Marine Geology
Ghent University
Krijgslaan 281 S8
9000 Ghent, Belgium
marc.debatist@ugent.be

Published Online 5 December 2018

[1] Also at Renard Centre of Marine Geology, Ghent University, Krijgslaan 281 S8, 9000 Ghent, Belgium.